Eksploatacja i Niezawodnosc - Maintenance and Reliability
Volume 29 (2027), Issue 1
https://ein.org.pl
The Polish Maintenance Society

Two-dimensional and three-dimensional numerical simulation study on the effect of rotor speed ratio on mixing performance in rubber compounding

Guolin Wang[1], Zhan Ni[1,*]

[1] School of Automotive and Traffic Engineering, Jiangsu University, Zhenjiang 212013, China
* Corresponding Author: nz335400@163.com

Received: 10 April 2026
Revised: 14 April 2026
Accepted: 9 May 2026
Online: 9 July 2026

Abstract

The uniformity and efficiency of rubber mixing directly affect the compound performance and product quality, while the rotor speed ratio is a key process parameter that determines the material flow, shear, and distribution state inside an internal mixer. To investigate the effect of different rotor speed ratios on rubber mixing performance, this study establishes two-dimensional and three-dimensional internal mixing models based on the finite element numerical simulation method. The VOF two-phase flow model is employed to describe the rubber–air interface, and the Bird–Carreau model is used to characterize the non-Newtonian rheological behavior of rubber. A comparative analysis of the mixing processes is conducted under three operating conditions with speed ratios of 1, 1.15, and 1.25. The dispersive and distributive mixing characteristics under different speed ratios are evaluated using indicators such as pressure field, volume fraction distribution, cumulative probability of maximum shear stress, mixing index, average stretching length, and distribution index. The results show that, within the range investigated in this study, a speed ratio of 1.15 exhibits the best performance in terms of pressure distribution uniformity, material renewal capability, and overall mixing performance. The two-dimensional and three-dimensional models show good consistency in the variation trends of all indicators, while the three-dimensional model can more realistically reflect the pressure levels and spatial stretching effects. The findings of this study provide a reference for optimizing rotor speed ratios in rubber mixing processes and for applying two-dimensional models in preliminary parameter screening.

Keywords: *finite element, mixing, rotor speed ratio, three-dimensional model, two-dimensional model*

Article citation:
Wang G, Ni Z, Two-dimensional and three-dimensional numerical simulation study on the effect of rotor speed ratio on mixing performance in rubber compounding, Eksploatacja i Niezawodnosc – Maintenance and Reliability 2027: 29(1) http://doi.org/10.17531/ein/221637

Highlights

- The effect of the speed ratio on the quality of the mixing process was investigated.
- The results were cross-validated using both two-dimensional and three-dimensional models.
- This provides a basis for optimising operating conditions for rubber compounding.
- An analysis of flow field changes during the rubber compounding process.

1. Introduction

Rubber mixing is a critical process in the manufacturing of rubber products, and the quality of mixing directly affects the mechanical properties, processability, and final product consistency of the compound. During the mixing process, materials undergo complex shear, elongation, folding, and compaction within the internal mixer; therefore, process parameters play a role in determining the mixing performance [1]. Among these parameters, the rotor speed ratio alters the material renewal frequency, local shear intensity, and pressure distribution within the mixing chamber, thereby influencing both dispersive and distributive mixing performance. The reasonable selection of rotor speed ratio is of great significance for improving mixing uniformity, reducing energy consumption, and enhancing product quality.

In recent years, with the development of Computational Fluid Dynamics (CFD), numerical simulation has become an important tool for studying the rubber mixing process. Existing studies have mainly focused on the following aspects:

(1) Effect of filling factor on mixing flow field and mixing

performance

Dhakal et al. [2] were the first to simulate rubber mixing under fully filled and partially filled conditions using a two-dimensional computational fluid dynamics method. Liu et al. [3] conducted numerical simulations on the flow of rubber compounds in a partially filled internal mixer. Dhakal et al. [4] found that a partially filled mixing chamber exhibits superior performance in both dispersive and distributive mixing compared to a fully filled one. Ahmed et al. [5] reported that the optimal dispersive and distributive mixing characteristics are achieved when the filling factor ranges from 70% to 80%. Das et al. [6] carried out a series of three-dimensional CFD simulations with different filling factors in the mixing chamber and concluded that a filling factor of 75% provides the best distributive mixing performance. Puklia et al. [7] performed a three-dimensional non-isothermal simulation to investigate the effect of rotor speed ratio under partially filled rubber mixing conditions.

(2) Coupled behavior of flow field and temperature field under isothermal and non-isothermal conditions

Wang et al. [8] proposed a non-isothermal numerical simulation method. Liu Tianlei et al. [9] used the finite element analysis software POLYFLOW to perform a three-dimensional isothermal simulation of the mixing behavior in a twin-rotor continuous mixer, and comparatively analyzed the effects of fluid velocity, shear rate, and mixing index in the mixing section flow field on mixing performance. Pudyar et al. [10] found that there are significant differences between isothermal and non-isothermal simulations, highlighting the importance of the isothermal assumption. Liu Jinping et al. [11] conducted a three-dimensional non-isothermal and unsteady numerical simulation of polymer mixing in a Haake internal mixer using the computational fluid dynamics software ANSYS Fluent, obtaining the transient temperature distribution of the three-dimensional flow field and analyzing the heat transfer between mixing chambers.

(3) Effects of rotor structural parameters and operating conditions on flow field distribution and mixing performance

Ping Fu et al. [12] employed an orthogonal experimental method to investigate a self-developed rubber compound formulation and determined the optimal mixing parameters. Salahudeen et al. [13] studied the optimization of rotor speed in a non-intermeshing batch internal mixer based on elongation, efficiency, and viscous heating. Lü Dawei et al. [14], from the perspective of computational fluid dynamics, verified that the mixing performance pattern of the internal mixer does not change with variations in material status. Liu Genchun et al. [15] conducted mixing experiments under different process parameters at rotor phase angles of 0° and 180°, respectively, and obtained the optimal process conditions.

(4) Applicability of two-dimensional and three-dimensional models in mixing process simulation

Wang Chuansheng et al.[16] conducted three-dimensional dynamic simulations of the mixing flow field in a synchronous rotor internal mixer with different initial phase angles, based on the viscoelastic fluid simulation software POLYFLOW. Zhai Tianjian et al.[17]performed dynamic simulations of the internal mixing process using a coupled finite element and discrete element method. Wang Chuansheng et al. [18] also carried out a finite element analysis of the temperature field distribution of a three-dimensional synchronous internal mixer rotor during the mixing process. Wang et al. [19] compared the results of two-dimensional and three-dimensional computational models at different rotational speeds, investigating the differences between these models in rubber mixing CFD simulations.

However, existing studies still show limitations regarding rotor speed ratio: first, most research focuses on a single model or operating condition, lacking systematic comparisons between two-dimensional and three-dimensional models; second, the applicability of two-dimensional models in rotor speed ratio optimization remains unclear; third, analyses of speed ratio effects are often limited to flow field descriptions, with insufficient comprehensive evaluation of both dispersive and distributive mixing. In addition, the engineering significance of different rotor speed ratio values requires further clarification.

Based on this, this study establishes two-dimensional and three-dimensional numerical models of an internal mixer and conducts a comparative analysis of the mixing processes under identical conditions with rotor speed ratios of 1, 1.15, and 1.25. The mixing performance under different speed ratios is systematically evaluated using indicators such as pressure field, volume fraction distribution, cumulative probability of

maximum shear stress, mixing index, average stretching length, and distribution index. Furthermore, the differences between the two-dimensional and three-dimensional models in terms of result trends and engineering applicability are analyzed. The findings provide a reference for optimizing rotor speed ratios and selecting appropriate modeling approaches.

2. Geometric structure and materials

The geometric model employed in this study is a mixer chamber comprising two shear-type rotors rotating in opposite directions: the left rotor rotates clockwise, while the right rotor rotates counterclockwise. The three-dimensional model is shown in Fig.1(a), and the two-dimensional model in Fig.1(b). Since both rubber and air are present within the mixer chamber, a multiphase flow VOF model [14] was adopted.

$$\frac{\partial C_i}{\partial t} + Vg\nabla C_i = 0 \tag{1}$$

The volume fraction of phase *i* is governed by.

Under a 75% fill factor condition, the main material is rubber. Its material parameters were experimentally measured and fitted before being input into the Bird–Carreau model to define viscosity.

Rubber is regarded as an incompressible shear-thinning non-Newtonian fluid, exhibiting pseudoplastic behaviour under high shear rates and Newtonian behaviour under low shear rates. The relationship between viscosity and shear rate is described by the Bird–Carreau model [20]:

$$\eta(\dot{\gamma}) = \eta_\infty + (\eta_0 - \eta_\infty)[1 + (\lambda\dot{\gamma})^2]^{\frac{n-1}{2}} \tag{2}$$

Table 1. Rheological Properties of Rubber.

Parameter	Value	Unit
Zero shear viscosity	117631.7	Kg/ (m s)
Infinite shear viscosity	4.55×e^{-7}	Kg/ (m s)
Time constant	5.537	s
Flow index	0.159	—

In the equation,$\eta(\dot{\gamma})$ is the viscosity at shear rate $\dot{\gamma}$; η_0 is the limiting viscosity at zero shear rate;η_∞ is the limiting viscosity at high shear rate; λ is the time constant, reflecting the characteristic time of the fluid's response to changes in shear rate; n is the flow index, used to describe the shear thinning behaviour of the fluid. When 0 < n < 1, this model effectively reflects the viscosity decrease characteristics of shear-thinning fluids in the medium to high shear rate range, making it suitable for analysing the rheological behaviour of polymer materials and rubber matrices. Specific parameters are shown in Table 1.

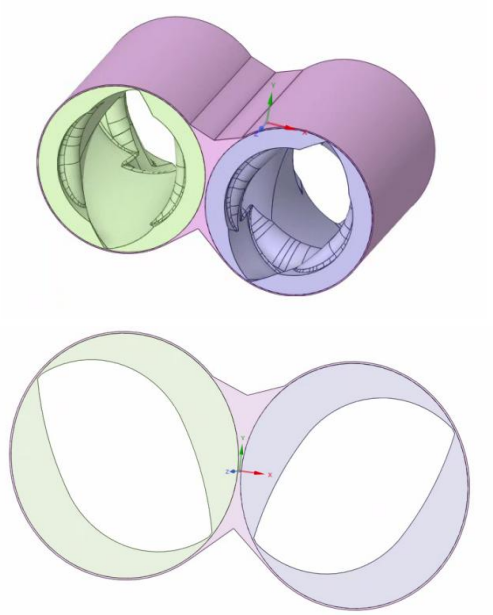

Figure 1. Three-dimensional model and two-dimensional model of the mixing chamber.

3. Fundamental equations

1 Mass Conservation Equation

$$\frac{\partial \rho}{\partial t} + \nabla \cdot (\boldsymbol{\rho}\mathbf{v}) = \mathbf{0} \tag{3}$$

where ρ is density (kg/m³) and v is velocity vector (m/s).

2. Momentum Conservation Equation

$$\rho\left(\frac{\partial v}{\partial t} + \mathbf{v}\cdot\nabla\mathbf{v}\right) = -\boldsymbol{\nabla}\mathrm{p} + \boldsymbol{\nabla}\cdot\tau + \rho\mathrm{g} \tag{4}$$

where p is pressure (Pa), τ is the stress tensor (Pa), and g is gravitational acceleration (m/s²).

3. Species Transport Equation (Material Diffusion)

$$\frac{\partial C_i}{\partial t} + \nabla \cdot (C_i\mathbf{v}) = \nabla \cdot (D_i\nabla C_i) + R_i \tag{5}$$

where c_i is concentration of component i, D is diffusion coefficient, and R_i is reaction rate. As this study considers isothermal conditions, the energy equation is neglected.

4. Research methods

4.1. Numerical model and computational method

To investigate the effect of different rotor speed ratios on the rubber mixing process, this study establishes two-dimensional and three-dimensional internal mixing models based on the Computational Fluid Dynamics method. During mixing, rubber behaves as a highly viscous, shear-thinning non-Newtonian fluid; therefore, the Bird–Carreau model is employed to

describe its rheological properties, and the rubber is assumed to be incompressible. Considering the high viscosity and low Reynolds number of the rubber system, the mixing process is dominated by viscous shear effects; thus, a laminar flow model is adopted for the simulation.

To describe the evolution of the interface between rubber and air within the mixing chamber, the VOF (Volume of Fluid) two-phase flow model is used. The geometric model is appropriately simplified while retaining key features such as the main structure of the mixing chamber, rotor profiles, and the meshing region, to reduce computational cost while ensuring the accuracy of the primary flow and mixing characteristics.

4.2. Operating parameters and boundary conditions

This paper simulates the mixing process under isothermal conditions to highlight the influence of the rotor speed ratio on flow and mixing behavior. The initial filling ratio is set at 75%, as shown in Figure 2. This operating condition represents a typical partially filled state commonly used in rubber mixing; it ensures that the material is fully subjected to shearing and renewal whilst retaining sufficient free space to observe the evolution of the flow process.

The speed of the left rotor was set to 44 r/min as the reference operating condition; the speed of the right rotor was set to 44 r/min, 50.6 r/min and 55 r/min respectively, corresponding to speed ratios of 1, 1.15 and 1.25. Here, a speed ratio of 1 represents synchronous rotation, 1.15 characterizes common moderate speed difference conditions, and 1.25 is used to analyses the effect of higher speed differences on mixing behavior.

The rotor surface is defined as a rotating moving wall, whilst the walls of the mixing chamber are fixed, non-slip boundaries. A transient solution method is employed, with a time step of 0.0005 s; this step size ensures computational stability whilst effectively capturing transient flow changes during rotor motion. The total simulation duration is 24 s to cover the main evolutionary stages of the mixing process.

In the numerical solution, the pressure–velocity coupling utilized the SIMPLEC algorithm, pressure discretization employed the PRESTO! scheme, and the momentum equations were discretized using a second-order scheme to enhance computational accuracy. The specific settings are shown in Table 2.

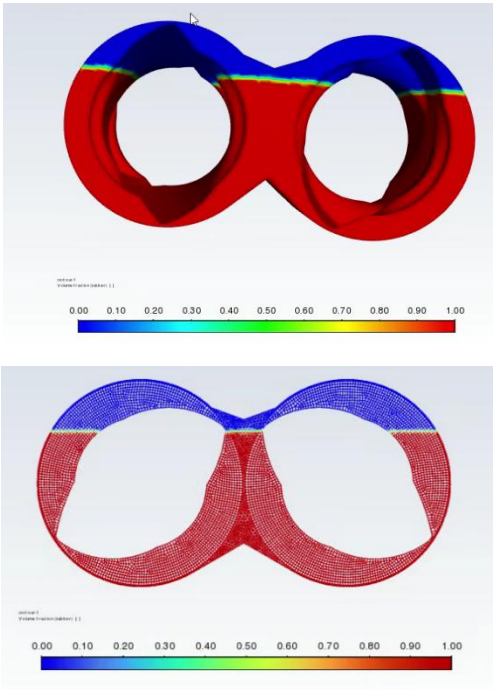

Figure 2. Initial rubber distribution diagrams in two and three dimensions.

Table 2. Numerical Simulation Settings for Compounding

Parameters	Value	Parameters	Value
Filling factor	75%	Solver	Transient
Left rotor speed	44 r/min	Pressure-velocity coupling	SIMPLEC
Speed ratio	1 / 1.15 / 1.25	Pressure discretization	PRESTO!
Time step	0.0005 s	Momentum discretization	Second-order
Total time	24 s		

4.3. Grid Partitioning and Irrelevance Analysis

To verify that the mesh size does not affect the computational results, eight monitoring points were randomly selected within the fluid domain of the three-dimensional simulation to investigate the velocity distribution at these points under different mesh sizes, as shown in Figure 3. The results indicate that when the mesh size is less than 9 mm, the velocity results at each monitoring point remain largely consistent, suggesting that the computational results are insensitive to mesh size and that the numerical solution has reached a mesh-independent state. Furthermore, the trends observed in the two-dimensional model are consistent with those in the three-dimensional model. Therefore, based on a balance between computational accuracy and computational cost, a 7 mm mesh size was selected for subsequent simulations. The mesh model is shown in Figure 4.

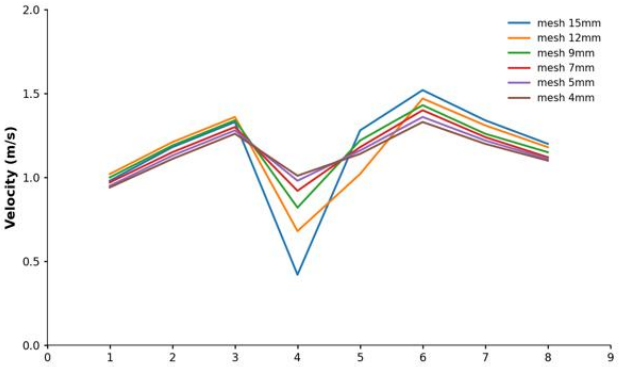

Figure 3. Grid-independent testing.

Three-dimensional grid model

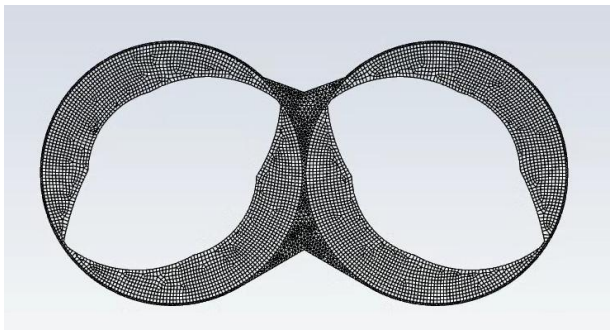

Three-dimensional grid model

Figure 4. Grid model.

4.4. Evaluation criteria

In the rubber mixing process, mixing mechanisms can be categorized into two types: distribution mixing and dispersion mixing. Distribution mixing aims to achieve spatial uniform distribution of different materials throughout the mixing chamber, primarily relying on stretching, folding, and macro-scale flow structures. Dispersion mixing, on the other hand, focuses on breaking down filler agglomerates into micron- or even nanometer-scale particles through localized high shear and high stress. In this study, particle tracking was used to analyses filler concentration distribution, and the mixing index was calculated to evaluate the effectiveness of distribution mixing. Additionally, shear rate, stress field, and energy dissipation rate analyses were employed to assess dispersion mixing capability, providing theoretical support for optimizing the mixing process.

(1) Cumulative probability distribution of maximum shear stress [21]: This refers to the maximum shear stress experienced by particles throughout the mixing process. When rubber particles undergo a single instance of high shear stress during mixing, there is a high probability that large rubber particles will break down into smaller particles, which is known as the fragmentation and dispersion of rubber particles. The cumulative probability of maximum shear stress is calculated by statistically analysing the maximum shear stress experienced by all tracer particles throughout the mixing process and summing the probabilities of the maximum shear stress experienced by all particles. The mechanism of agglomerate fragmentation is generally believed to be proportional to the shear stress applied, with the mathematical equation being:

$$\tau_{critical} \propto \frac{1}{R_0} \tag{6}$$

The cumulative distribution of maximum shear stress is obtained by statistically calculating the maximum shear stress experienced by each particle within 24 seconds, representing the percentage of particles in the particle group that experience maximum shear stress higher than the specified shear stress. The higher the percentage of particles, the stronger the ability of the flow field to decompose rubber and the better the dispersion and mixing characteristics.

(2) Mixing index [22]: To quantify the dispersion mixing

characteristics, the variable of the mixing index is introduced, and its mathematical equation is:

$$\lambda_{MZ} = \frac{|D|}{|D| + |\omega|} \quad (7)$$

Where |D| is the magnitude of the deformation tensor and |ω| is the magnitude of the vorticity tensor. Typically, the mixing index value ranges from 0 to 1. When the mixing index value approaches 0, the flow is purely rotational; when it approaches 0.5, the flow is simple shear; and when it approaches 1, the flow is purely tensile. Research suggests that tensile flow demonstrates superior dispersion capability compared to shear flow.

(3) Average stretch length [23]: To quantify the distribution mixing characteristics, Ottino defined the average stretch length (LOS) to quantify the distribution mixing effect. The average stretch length represents the ratio of the distances between different particle pairs and can be obtained from the output particle group position coordinates. The mathematical equation for the average stretch length is:

$$L_\lambda = \frac{|\chi_t|}{|\chi_o|} \quad (8)$$

Where χ_o and χ_t represent the distance between arbitrary particle pairs at the initial time and time t, respectively. As the mixing time increases, the particle group is affected by the rotor movement and gradually disperses to various areas of the mixing chamber, so the value of increases continuously with time. The larger the average elongation value, the higher the degree of dispersion of the particle group, i.e., the better the distribution and mixing characteristics.

(4) Distribution index [24]: Another indicator for evaluating the mixing ability of the flow field distribution is the cluster distribution index, which is obtained by comparing the particle distribution at each moment with the ideal particle distribution. The ideal particle distribution refers to the cluster distribution index curve when the particle cluster is uniformly distributed in the mixing chamber. The cluster distribution index can be used to evaluate the difference between the particle distribution and the ideal distribution under various filling coefficients. Its data equation is:

$$f(r) = \frac{2}{N(N-1)} \sum_i \delta(r_i' + r)\delta(r_i') = \int_{r-\frac{\Delta r}{2}}^{r+\frac{\Delta r}{2}} c(r)dr \quad (9)$$

Where f(r) is the correlation function coefficient between particle pairs, representing the probability of finding a neighboring particle within the range of r-Δr/2 to r+Δr/2 for the i-th particle. If the particle exists, then δ_r=1; if it does not exist, then δ_r=0, and c(r) is the probability density function. The area enclosed by the c(r) curve and the x-axis is always 1. The mathematical equation for c(r) is:

$$\sum_{r=0}^{r=r_{max}} c(r)\Delta r = 1 \quad (10)$$

Where r_{max} is the maximum distance in the mixing chamber. Therefore, when the distance is greater than r_{max}, no particles will be found. That is, c(r>r_{max})=0. Therefore, the cluster distribution index (CDI) can be obtained through the following mathematical equation:

$$\varepsilon = \frac{\int_0^\infty [c(r) - c(r)_{ideal}]^2 dr}{\int_0^\infty [c(r)_{ideal}]^2 dr} \quad (11)$$

Among them, c(r) is the distribution calculated under different conditions, and $c(r)_{ideal}$ is the ideal distribution. ε is the value of the cluster distribution index (CDI). During the initial mixing period, the value of ε will be large because the particles are heavily aggregated. As time changes, the value of ε will become smaller, approaching the ideal distribution.

5. Results and discussion

Rubber mixing involves a certain rotor speed ratio, and different rotor speed ratios have varying effects on the mixing results. Generally, the optimal rotor speed ratio is between 1 and 1.25. Therefore, this paper selects three different speed ratios to analyze the changes in flow field and particle-related parameters, comparing and discussing the mixing results under the three speed ratios to determine the optimal speed ratio.

Simulation settings: Two-dimensional and three-dimensional models were used, with speed ratios set to 1, 1.15, and 1.25. Simulation conditions: For the two-dimensional/three-dimensional model, the left rotor speed is 44 r/min, and the right rotor speed is multiplied by the speed ratio value. The filling factor is set to 75%, and the conditions are isothermal. With a termination time of 24 seconds, the

distribution characteristics and dispersion characteristics of the rubber compound after 24 seconds of mixing under different rotor speed ratio conditions are analyzed and compared.

5.1. Flow field analysis

During the rubber mixing process, the rubber compound undergoes forced stirring by the rotor in the mixing chamber, exhibiting complex non-Newtonian flow behavior accompanied by intense shear, stretching, and temperature rise effects. Flow field distribution, as a key physical characteristic in the mixing process, directly determines the uniformity of material dispersion, mixing efficiency, and the final properties of the rubber compound. Therefore, conducting an in-depth analysis of the flow field characteristics during the mixing process is of great significance for elucidating the mechanisms by which different process parameters influence mixing performance.

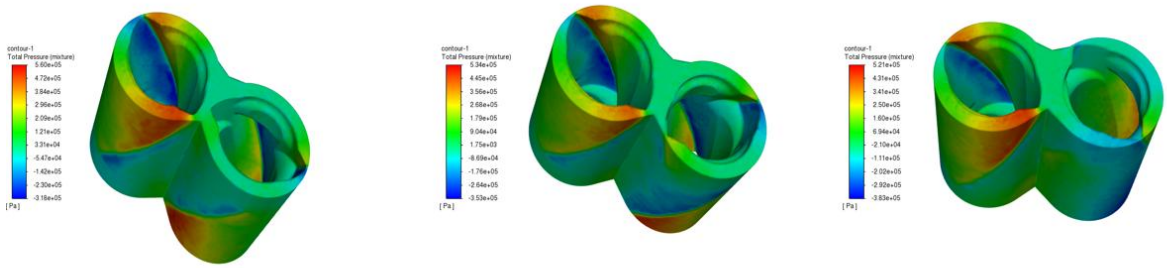

Three-dimensional model pressure field distribution

Pressure field distribution at the cross-section at Z=500 mm in the three-dimensional model

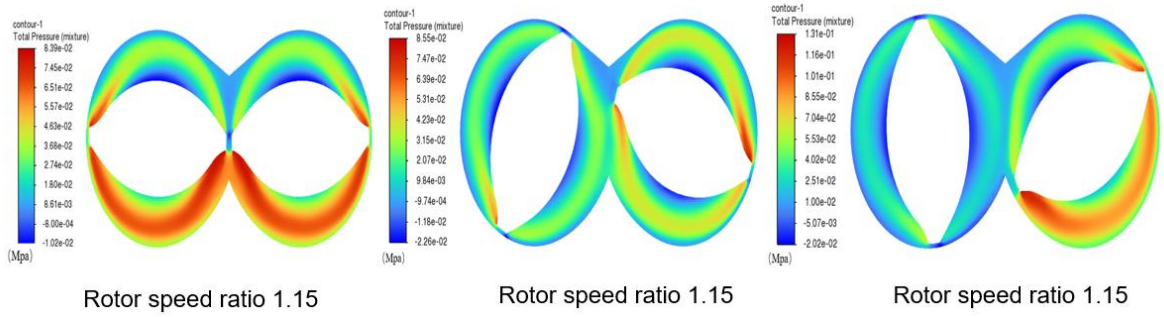

Two-dimensional model pressure field

Figure 5. Pressure field distribution of three-dimensional and two-dimensional models at different speed ratios.

5.1.1. Pressure field analysis

As shown in Figure 5, significant differences in the pressure field distribution within the mixing chamber can be observed under different rotor speed ratios. Overall, high-pressure regions are mainly concentrated at the leading edges of the rotors and in the meshing zone, where the material experiences the most intense compaction and shear effects.

When the speed ratio is 1, the pressure distribution within the chamber is relatively dispersed, and the high-pressure regions are limited in extent, indicating that the rotors exert relatively weak compaction and driving effects on the material. As the speed ratio increases to 1.15, the high-pressure regions

expand significantly and become more uniformly distributed. This suggests that a moderate speed difference enhances the material renewal frequency and stress level within the chamber, which is beneficial for improving compaction and dispersive mixing performance.

When the speed ratio is further increased to 1.25, although the local pressure level remains high, the high-pressure regions exhibit a certain degree of concentration, and the spatial uniformity decreases. This indicates that an excessive speed difference may lead to overly strong local stresses, thereby affecting the overall stability of the mixing process.

In summary, within the range investigated in this study, a speed ratio of 1.15 not only increases the pressure level but also maintains good spatial uniformity, making it more favorable for stable mixing. This result is consistent with the subsequent analyses of volume fraction distribution and mixing evaluation indices, further demonstrating that an appropriate speed difference contributes to the overall improvement of mixing performance.

5.1.2. Volume fraction

Figure 6 shows the distribution of rubber volume fraction under different rotor speed ratios. The volume fraction distribution reflects the filling state and renewal capability of the material within the mixing chamber.

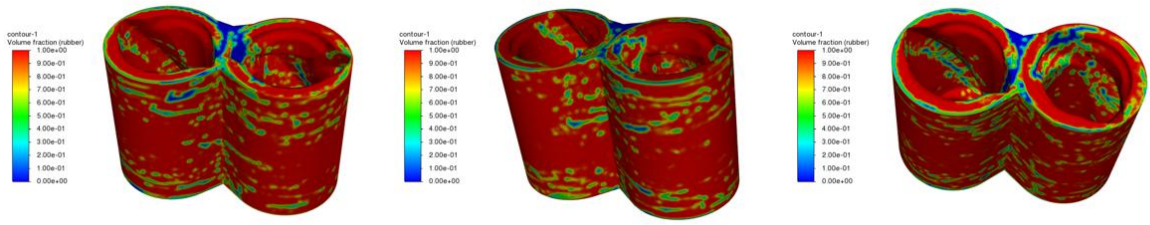

Volume fraction distribution of three-dimensional models

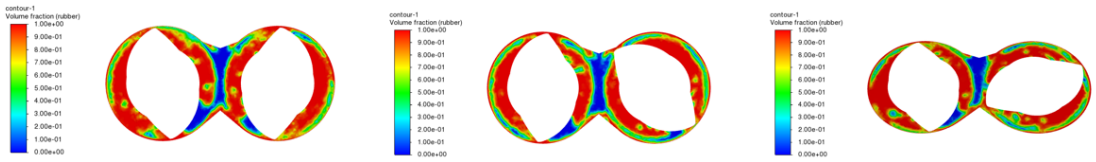

Volume fraction distribution of the cross-section at Z=500 mm in the three-dimensional model

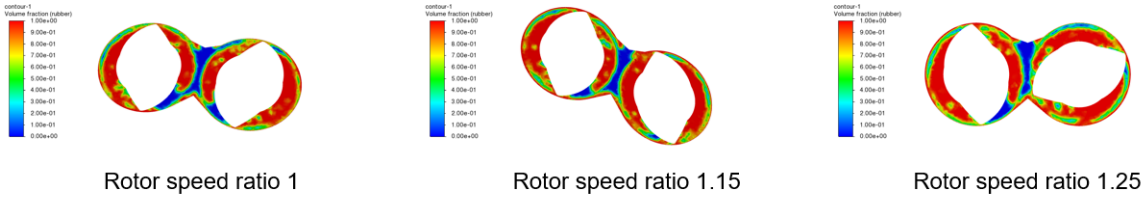

Two-dimensional model volume fraction distribution

Figure 6. Volume fraction distribution of three-dimensional and two-dimensional models at different speed ratios.

At a speed ratio of 1, although the chamber is generally in a high-volume fraction state, there are still noticeable low-volume-fraction regions locally, indicating insufficient material renewal and the tendency to form localized stagnant zones. As the speed ratio increases to 1.15, the high-volume-fraction regions become more continuous, and the low-volume-fraction regions are significantly reduced. This suggests that material renewal and spreading within the chamber are more sufficient, leading to improved distribution uniformity.

When the speed ratio is further increased to 1.25, although the high-volume-fraction regions continue to expand, some areas exhibit discontinuous or scattered distributions. This

indicates that an excessive speed difference may lead to unstable flow paths, thereby affecting the overall distribution uniformity.

Therefore, from the perspective of volume fraction distribution, a speed ratio of 1.15 enhances the filling capability while maintaining good uniformity, demonstrating superior distributive mixing characteristics. This result is consistent with the pressure field distribution and the trends of subsequent mixing indices, further confirming that a speed ratio of 1.15 has advantages in improving the spatial distribution of the material.

5.2. Dispersion mixing

(1) Cumulative probability distribution of maximum shear stress: Use evaluation indicators to obtain the cumulative probability distribution of maximum shear stress under different speed ratios after 24 seconds of mixing, as shown in Fig.7.

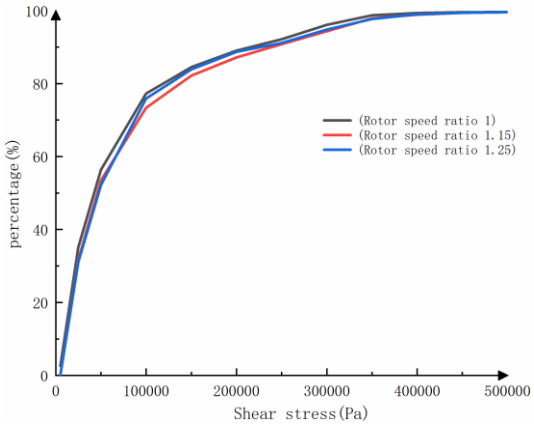

(a)

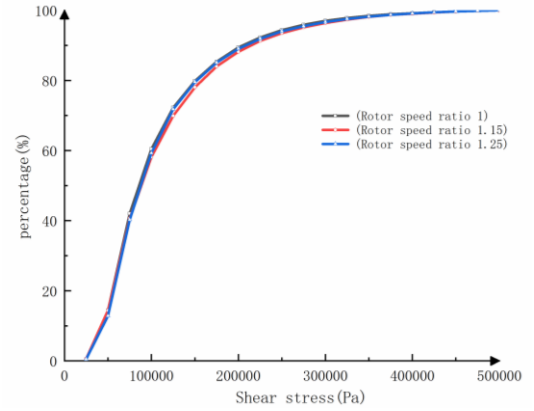

(b)

Figure 7. Cumulative probability distribution of shear stress under different speed ratios in a two-dimensional model (a), Cumulative probability distribution of shear stress under different speed ratios in a three-dimensional model (b).

As shown in Figure 7, the cumulative probability distributions of the maximum shear stress of particles under different rotor speed ratios exhibit similar overall trends, but differences are observed in the medium shear stress range. Compared with speed ratios of 1 and 1.25, the curve corresponding to a speed ratio of 1.15 is smoother, indicating that the shear experienced by particles during the mixing process is more uniformly distributed under this condition. This contributes to improving overall dispersive mixing performance while avoiding excessively high local share.

(2) Mixing index: Use evaluation indicators to obtain the mixing index under different speed ratios after 24 seconds of mixing, as shown in Fig.8.

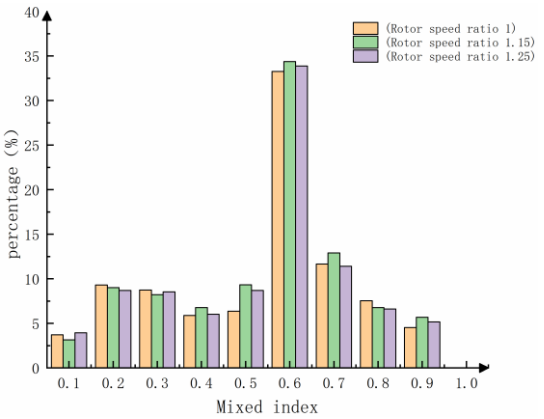

(a)

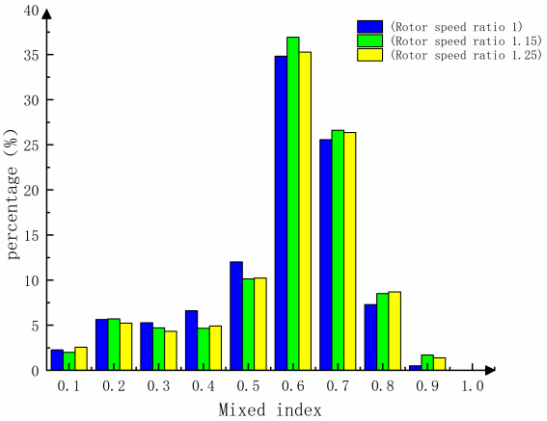

(b)

Figure 8. Mixed index of different speed ratios in a two-dimensional model (a) and mixed index of different speed ratios in three-dimensional models (b).

Figure 8 shows the distribution of the mixing index under different rotor speed ratios. In general, a mixing index closer to 1 indicates stronger extensional deformation in the flow field, and extensional flow is beneficial for enhancing dispersive mixing performance.

The results show that, at a speed ratio of 1.15, a relatively high proportion of values falls within the 0.6–0.7 range, indicating that a larger fraction of the flow field exhibits combined shear and extensional effects, which is favorable for improving the mixing performance. In comparison, at a speed ratio of 1, the distribution is mainly concentrated in lower mixing index ranges, suggesting weaker mixing effects. Although the speed ratio of 1.25 shows some improvement in higher-value regions, its overall distribution is less concentrated than that of 1.15.

5.3. Distribution mixture

(3) Average elongation: Use evaluation indicators to obtain the average elongation under different speed ratios after 24 seconds of mixing. Use the processed average elongation, as shown in Fig.9.

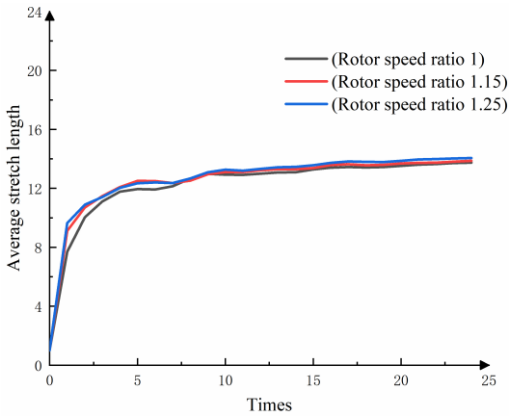

(a)

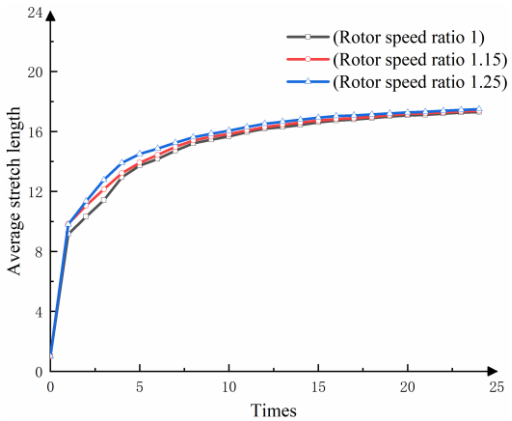

(b)

Figure 9. Average elongation at different speed ratios in a two-dimensional model (a) and average elongation at different speed ratios for the three-dimensional model (b).

Figure 9 shows the variation of the average stretching length with time. It can be observed that the average stretching length increases over time under all rotor speed ratios, but the growth rates differ.

The speed ratio of 1.15 exhibits a relatively higher average stretching length throughout the entire mixing process, indicating that this condition can more effectively promote material stretching and unfolding, thereby enhancing distributive mixing capability. In comparison, the speed ratio of 1 shows a slower increase. Although the speed ratio of 1.25 increases more rapidly in the early stage, it tends to stabilize in the later stage, and its overall performance is slightly inferior to that of 1.15.

(4) Distribution index: Use evaluation indicators to obtain the distribution index under different speed ratios after 24 seconds of mixing, as shown in Fig.10.

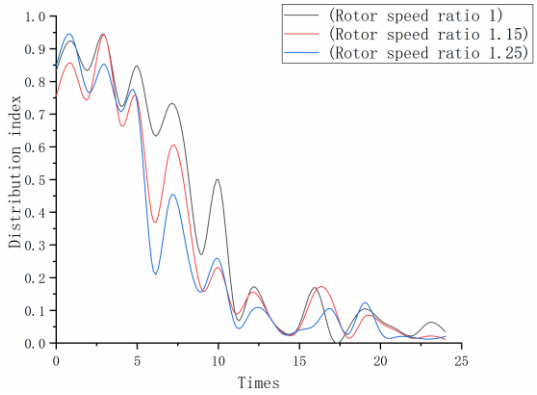

(a)

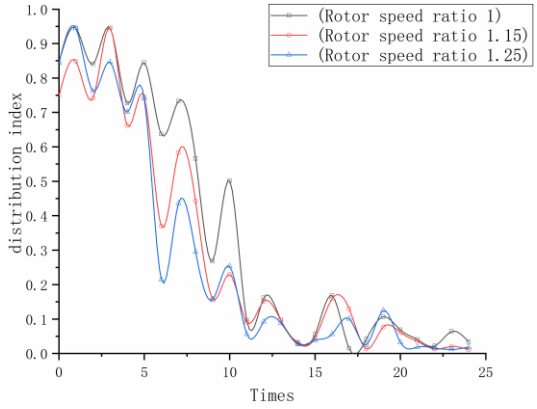

(b)

Figure 10. Distribution index of different speed ratios in a two-dimensional model (a) and distribution index of different speed ratios in the three-dimensional model (b).

As shown in Figure 10, the distribution index generally decreases with time, indicating that the material gradually becomes more uniformly distributed during the mixing process. Compared with different rotor speed ratios, the speed ratio of 1.15 exhibits a lower distribution index in both two-dimensional

and three-dimensional models and reaches a stable state earlier, demonstrating better performance in promoting uniform material distribution.

Overall, the results indicate that the effect of rotor speed ratio on mixing performance shows consistent trends across multiple evaluation indicators. The speed ratio of 1.15 outperforms the other operating conditions in terms of pressure distribution uniformity, volume fraction continuity, and mixing index performance. This suggests that an appropriate speed difference can enhance material stress and renewal capacity while avoiding non-uniformity caused by excessively strong local shear. In contrast, the speed ratio of 1 shows insufficient mixing, while the speed ratio of 1.25 improves local interaction intensity but reduces overall uniformity. Therefore, from a multi-indicator consistency perspective, the speed ratio of 1.15 exhibits the best overall mixing performance within the scope of this study. These results demonstrate that multi-indicator joint analysis is important for revealing the mechanisms of the mixing process and optimizing process parameters. Meanwhile, the consistency of trends between the two-dimensional and three-dimensional models further indicates that the two-dimensional model can be used for preliminary parameter screening, while the three-dimensional model offers higher reliability for detailed analysis.

It should be noted that this study still has certain limitations. First, the simulations were conducted under isothermal conditions, without considering the feedback effect of viscous heating and temperature rise on the rheological properties of rubber. Second, the model does not incorporate the dynamics of filler particle breakage and agglomeration, so the evaluation mainly reflects the macroscopic flow-field-based mixing performance. In addition, only a filling factor of 75% and three speed ratios (1, 1.15, and 1.25) were investigated; therefore, the applicability of the conclusions still needs to be further validated through a wider parameter range and experimental results.

6. Conclusion

Based on the Computational Fluid Dynamics method, this study establishes two-dimensional and three-dimensional rubber internal mixing models and systematically compares three operating conditions with rotor speed ratios of 1, 1.15, and 1.25. The following conclusions are drawn:

(1) The rotor speed ratio has a significant influence on rubber mixing performance. As the speed ratio increases from 1 to 1.15, the pressure distribution, material filling state, and both dispersive and distributive mixing performance in the mixing chamber are improved. When the speed ratio is further increased to 1.25, although local shear and filling effects are further enhanced, more pronounced local non-uniformities also occur. Considering all evaluation indices, a speed ratio of 1.15 exhibits the best overall mixing performance within the scope of this study.

(2) The two-dimensional and three-dimensional models show good consistency in the trends of pressure field, volume fraction distribution, and various evaluation indices, indicating that the two-dimensional model can be used for rapid preliminary screening of process parameters such as rotor speed ratio. However, the three-dimensional model can further capture three-dimensional effects such as axial stretching, end-flow behavior, and realistic pressure levels, making it more advantageous for detailed analysis and engineering applications.

(3) This study reveals the influence mechanism of rotor speed ratio on mixing performance from both pressure field analysis and multi-index evaluation perspectives, providing a theoretical reference for optimizing rotor speed ratio in internal mixers. It should be noted that this work is based on isothermal conditions and a limited range of operating cases; therefore, further studies incorporating non-isothermal simulations, broader parameter combinations, and experimental validation are needed to refine and improve the conclusions.

References

1. Zhu B. Current Status and Development Prospects of the Domestic Rubber Compounding Industry. *China Rubber* 2021; (4): 30.
2. Dhakal P, Das S R, Poudyal H. Numerical simulations of partially filled rubber mixing in a 2-wing rotor-equipped chamber. *Journal of Applied Polymer Science* 2016;b133(48): 44250.

3. Fu P , Bai F B , Wang C S.Optimize Mixing Process Parameters of Synchronous Rotor Mixer Based on Orthogonal Method.*Key Engineering Materials* 2012; 501: 442-447. DOI:10.4028/www.scientific.net/KEM.501.442.
4. Wang G L, Wang Y. Research on non-isothermal numerical simulation algorithm for tire rubber mixing based on multiphase flow decoupling principle. *International Journal of Automotive Technology* 2024; 26(3): 1-12.
5. Liu J P, Li F Z, Zhang L Q. Numerical simulation of flow of rubber compounds in partially filled internal mixer. *Journal of Applied Polymer Science* 2015; 132(35): 42452. doi: 10.1002/app.42452.
6. Liu T L, Du Y X. Simulation of mixing behaviour based on POLYFLOW twin-screw continuous mixing machine. *Modern Plastics Processing and Applications* 2010; (5): 15-18. doi: 10.3969/j.issn.1004-3055.2010.05.007.
7. Salahudeen S A, Alothman O, Elleithy R H. Optimization of rotor speed based on stretching, efficiency, and viscous heating in no intermeshing internal batch mixer: simulation and experimental verification. *Journal of Applied Polymer Science* 2012; 127(5): 4229-4238. doi: 10.1002/app.37592.
8. Lv D W, Zhu X Z, Xin Y Y. Analysis of the movement and mixing performance of particles in an internal mixer. *Plast* 2020; 49(3): 54-58.
9. Wang C S, Zhang L, Zhai T J. Finite element simulation analysis of the mixing flow field of synchronous rotor internal mixers with different initial phase angles. *China Rubber Ind* 2019; 66(6): 408-413.
10. Zhai T J. Simulation and visualisation of the mixing process in a closed mixer. Qingdao (China): Qingdao University of Science and Technology; 2019.
11. Wang K, Liu H, Chang T. Numerical optimization simulation of synchronous four-wing rotor. *Materials* 2020; 13(23): 5353. doi: 10.3390/ma13235353.
12. Ahmed I, Chandy AJ, Poudyal H. Three-dimensional numerical investigations of the effect of fill factor on dispersive and distributive mixing of rubber under non-isothermal conditions. *Polymer Engineering and Science* 2019; 59(3): 535-546. doi: 10.1002/pen.24963.
13. Dhakal P, Das S R, Poudyal H. Investigation of fill factor in two-wing rotor mixing of rubber by using computational fluid dynamics. *Tire Science and Technology* 2017; 45(2): 144-160. doi: 10.2346/tire.17.450202.
14. Poudyal H, Ahmed I, Chandy AJ. Three-dimensional, non-isothermal simulations of the effect of speed ratio in partially filled rubber mixing. *International Polymer Processing* 2019; 34(2): 219-230. doi: 10.3139/217.019022.
15. Connely R K, Kokini J L. 3D numerical simulation of the flow of viscous Newtonian and shear thinning fluids in a twin sigma blade mixer. *Advances in Polymer Technology* 2006; 25(3): 182-194. doi: 10.1002/adv.20071.
16. Wang C S, Zhang J L. Three-dimensional temperature field analysis of synchronous rotors in internal mixers. *China Rubber/Plastics Technol Equip* 2008; (5): 1-7.
17. Liu G C, Wang H Y, Chen R H. Experimental study on the mixing process of a 0.3 L internal mixer. *China Rubber/Plastics Technol Equip* 2021; 47(5): 1-6.
18. Liu J P, Li F Z, Yang H B. Non-isothermal numerical simulation study of the three-dimensional flow field of a Hakko mixer. *China Rubber Industry* 2016; (7): 429-433.
19. Wang G L, Wang J S, Zhou H C. Simulation method for rubber compounding under isothermal partial filling conditions. *Advances in Polymer Technology* 2023; 2023(1): 1-16. doi: 10.1155/2023/5571039.
20. Khan M W A, Salahuddin T, Chu Y M. Analysis of the Carreau fluid model presenting physical properties along different molecular axes near an anisotropic rough surface. *International Communications in Heat and Mass Transfer* 2021; 123: 105233. doi: 10.1016/j.icheatmasstransfer.2021.105233.
21. Poudyal H, Das S R, Chandy A J. Non-isothermal effects in partially filled rubber mixing simulations of manufacturing processes. *Rubber Chemistry and Technology* 2019; 92(1): 152-167. doi: 10.5254/rct.19.82590.
22. Cheng J J, Manas-Zloczower I. Flow field characterization in a Banbury mixer. *International Polymer Processing* 1990; 5(3): 178-183. doi: 10.3139/217.900178.
23. Ottino J M. The kinematics of mixing: stretching, chaos, and transport. Cambridge: *Cambridge University Press*; 1989.
24. Wong TH, Manas-Zloczower I. Two-dimensional dynamic study of the distributive mixing in an internal mixer. *International Polymer Processing* 1994; 9(1): 3-10. doi: 10.3139/217.940003.